RSC Advances

PAPER

View Article Online
View Journal | View Issue

Cite this: *RSC Adv.*, 2014, **4**, 25118

Tribological study of hydrolytically stable S-containing alkyl phenylboric esters as lubricant additives

Zhipeng Li,[ab] Yilin Li,[c] Yawen Zhang,[a] Tianhui Ren*[a] and Yidong Zhao[d]

Received 26th February 2014
Accepted 19th May 2014

DOI: 10.1039/c4ra01672f

www.rsc.org/advances

Three novel S-containing alkyl phenylboric esters, *i.e.*, DSPB, TSPB and TBPB, were prepared and characterized. Compared with common boric esters, these three additives exhibit significant hydrolytic stability, which can be attributed to their specific molecular structures, in which a phenyl group conjugates with an electron-deficient boron that helps improve the hydrolytic stability of boric esters. The tribological properties were evaluated using a four ball tester, which suggests that all the synthesized compounds act as anti-wear additives and have relatively high load-carrying capacities. In particular, it should be noted that, among the synthesized compounds, DSPB exhibits both anti-wear and friction-reducing properties. Furthermore, the worn surface was investigated by X-ray absorption near edge structure spectroscopy (XANES). The results demonstrate that the resulting tribofilm consists of trigonal and tetragonal coordination boron, iron sulfide and disulfide, and iron sulfate. Moreover, atomic force microscopy (AFM) was used to characterize the morphology of the tribofilm and the large pads elongated and orientated in the sliding direction were observed, which contribute to the anti-wear (AW) and extreme pressure (EP) performances.

1. Introduction

It is well known that base oil does not satisfy all the stringent requirements imposed on lubricants for use in heavy-duty machineries, such as modern engines, hydraulic devices and large construction vehicles, which usually release a significant amount of heat and exhibit severe material consumption in the joint working parts. Such friction-induced heat release and wear-induced material consumption accounts for about one-third of the world total energy consumption every year.[1,2] Various compounds containing boron, sulfur, phosphorus, halogens, nitrogen or metals as active components have been used as lubricating additives for base oil to minimize wear and control friction, and thus improve the working efficiency as well as prolong the lifetime of these heavy-duty machines. Zinc dialkyldithiophosphates (ZDDPs) have been widely used as lubricant additives in many heavy-duty machines.[3,4] However, there is a significant environmental risk in using ZDDPs because they produce zinc ash and large amount of sulfur and phosphorus compounds, which can cause air pollution by directly releasing these hazardous chemicals into the air or indirectly poisoning the emission-control catalysts and thus block the filters in car exhaust system.[5] Therefore, it is necessary to develop environmentally friendly lubricating additives to substitute or reduce the use of environmentally hazardous ZDDPs.[6]

Boron-containing additives have been reported to be promising alternatives for substituting ZDDPs due to their comparable mechanical lubricating properties as well as low environmental impact.[7] One of the typical boron-containing additives is organic boric esters, which are used because of their anti-oxidant properties as well as specific properties such as oil solubility, low-toxicity and biodegradability.[8,9] It has been reported that the formation of a thin layer of boric oxide (B_2O_3) on the metal surfaces under extreme pressure is responsible for its anti-wear properties.[10,11] Kapadia and co-workers proposed that amorphous networks of mixed three or four connective polymer units are formed on the metal surface due to the dehydration of H_3BO_3.[12] However, this process is still unclear and more effort is need to reveal the tribological behavior of boron on a metal surface.

Moreover, due to the electron deficiency of the boron atom, boric esters tend to hydrolyze under ambient conditions by forming the oil-insoluble and abrasive boric acid, which is considered as a major limitation for their further application.[13–15] A common method to improve the hydrolytic stability of boric esters is to introduce an electron-rich nitrogen atom

[a]*School of Chemistry and Chemical Engineering, Key Laboratory for Thin Film and Microfabrication of the Ministry of Education, Shanghai Jiao Tong University, 200240, China. E-mail: thren@sjtu.edu.cn; Tel: +86 21 5474 7118*

[b]*Laboratory of Solid Lubrication, Lanzhou Institute of Chemical Physics, Chinese Academy of Sciences, Lanzhou 730000, China*

[c]*Voiland School of Chemical Engineering and Bioengineering, Washington State University, Pullman, WA 99164, USA*

[d]*Beijing Synchrotron Radiation Facility, Institute of High Energy Physics, Chinese Academy of Sciences, Beijing 100039, China*

into the molecular structure, which can coordinate with boron for its stabilization.[7,15] Nevertheless, the N-containing boric esters still exhibit relatively poor hydrolytic stabilities due to the weakness of the coordination bond between boron and nitrogen. Therefore, it is necessary to develop a new strategy by molecule design to improve the hydrolytic stability of boric esters. In this report, we proposed an effective way to improve the hydrolytic stability of boric esters by introducing alkyl phenyl groups that are directly conjugated to the electron-deficient boron. The synthesized boric esters exhibit improved hydrolytic stabilities due to the p-π conjugating effect between the phenyl group and boron atom, and the long alkyl chain acts as a hydrophobic group that prevents a nucleophilic attack of water, which leads to hydrolysis. Moreover, S-containing borate esters have been extensively studied in lubricant oils.[5,13,16,17] It has been confirmed that a synergistic effect due to the formation of a protective film between S and B will occur when the element sulfur is introduced into the molecular structures of organic boric ester.[18] Therefore, three novel S-containing alkyl phenylboric esters were developed as lubricant additives and their tribological properties were evaluated. The results indicate that they all exhibit excellent anti-wear and friction-reducing properties as well as relatively high extreme pressure (EP) properties. We also believed that their unique tribological properties come from the specific tribological chemistry that occurs during the lubricating process under heavy-duty conditions. We utilized atomic force microscopy (AFM) and X-ray absorption near edge structure spectroscopy (XANES) to characterize the tribological surface at both a morphological level and a composition level and thus reveal the mechanism of the tribological chemistry.

2. Experimental

2.1 Base oil properties and synthesis of additives

A common mineral oil, hydro-isomerized and dewaxed base oil (HVI WH150, purchased from PetroChina Lanzhou Lubricating Oil R&D Institute in Lanzhou, China), was used as the base oil in this study without any further treatment. The physical properties of the HVIW H150 mineral oil are given in Table 1.

Table 1 Physical properties of the HVI WH150 mineral oil

Parameter	Value
Density (20 °C, g cm^{-3})	0.844
Kinematic viscosity (mm^2 s^{-1})	
40 °C	29.95
100 °C	5.512
Viscosity index	125
Chrominance number	0
Pour point (°C)	−30
Open flash point (°C)	226
Neutralizing value (mg KOH per g)	0.01
Extrinsic feature	Transparence
Evaporation loss, Noack 250 °C, 1 h (%)s	10.15

All chemicals (purchased from Shanghai Chemical Company, Shanghai, China) were of reagent grade and used without further purification. 4-Dodecylphenylboric acid was prepared according to procedures reported in previous studies.[19,20]

The synthesized additives are bis(1-(butylthio)propan-2-yl) 4-dodecylphenylboronate (TBPB), bis(1-(dodecylthio)propan-2-yl) 4-dodecylphenylboronate (DSPB) and bis(t-(dodecylthio) propan-2-yl) 4-dodecylphenylboronate (TSPB). The synthetic routes are shown in Fig. 1 and the related synthetic procedures can be described as follows:

Stoichiometric *n*-butanethiol (18.04 g, 0.20 mol), 1,2-epoxypropane (11.62 g, 0.20 mol) and triethylamine (20.24 g, 0.20 mol) as the catalyst were dissolved in 150 mL of dichloromethane in a 250 mL round-bottomed flask. The reaction mixture was stirred at room temperature overnight. The resulting reaction mixture was extracted with dichloromethane, acidified with dilute hydrochloric acid and washed with water 3 times. Then, the combined organic phases were dried over anhydrous $MgSO_4$ and filtered. The solvent was removed under reduced pressure to afford 1-(butylthio)propan-2-ol (26.24 g, 0.18 mol) in 89% yield.

4-Dodecylphenylboric acid (14.51 g, 0.05 mol), 1-(butylthio) propan-2-ol (14.83 g, 0.10 mol) and a catalytic amount of strong acid resin (Amberlite 732) were dissolved in 150 mL of toluene in a 250 mL round-bottomed flask equipped with a Dean–Stark trap for separation of water. The reaction mixture was refluxed for 6 h under a nitrogen atmosphere. The resulting reaction mixture was filtered and rotary evaporated to remove the toluene under vacuum resulting in TBPB (27.25 g, 0.05 mol) in 99% yield. DSPB (or TSPB) can be prepared by a reaction between *n*-dodecylmercaptan (or *t*-dodecylmercaptan) and 4-dodecylphenylboric acid using a similar procedure. All of the synthesized additives were characterized by infrared (IR) spectroscopy, nuclear magnetic resonance (NMR) and elemental analysis. The results of the elemental analysis are provided separately in Table 2 for the convenience of indicating the percentages of sulfur or boron, which are important parameters in subsequent discussion.

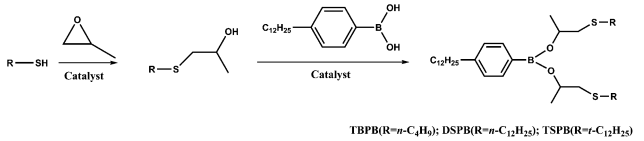

Fig. 1 Synthesis of S-containing alkyl phenylboric esters.

Table 2 Elemental analysis result of synthesized additives

Items	C (wt%)	H (wt%)	S (wt%)	B (wt%)
TBPB	69.37 (69.79)[a]	10.89 (10.80)[a]	11.66 (11.64)[a]	1.83 (1.96)[a]
DSPB	74.08 (74.37)[a]	11.99 (11.83)[a]	7.72 (8.27)[a]	1.36 (1.39)[a]
TSPB	74.04 (74.37)[a]	11.85 (11.83)[a]	7.90 (8.27)[a]	1.29 (1.39)[a]

[a] Calculated value (balanced by oxygen).

Bis(1-(butylthio)propan-2-yl) 4-dodecylphenylboronate (TBPB). Molecular formula: $C_{32}H_{59}BO_2S_2$. IR (KBr) (cm^{-1}): 2957.46m ($-CH_3$); 2926.53s, 2855.96m ($-CH_2-$); 1609.05w (C=C); 1457.08m, 1377.10m ($-CH_3$); 1341.85s ($-CH_2-$); 1310.81s (B–O); 758.54m (phenyl ring); 702.51w (C–B); 652.76w (C–S). ^{1}H-NMR (δ, ppm, $CDCl_3$): 7.69–7.09 (4H, phenyl ring), 2.72–2.34 (9H, alkyl chain), 1.58–1.22 (34H, alkyl chain), 0.93–0.80 (12H, alkyl chain).

Bis(1-(dodecylthio)propan-2-yl) 4-dodecylphenylboronate (DSPB). Molecular formula: $C_{48}H_{91}BO_2S_2$. IR (KBr) (cm^{-1}): 2953.72m ($-CH_3$); 2925.48s, 2854.45m ($-CH_2-$); 1609.35w (C=C); 1456.38m, 1377.10m ($-CH_3$); 1336.75s ($-CH_2-$); 1318.60s (B–O); 759.51m (phenyl ring); 701.27w (C–B); 652.43w (C–S). ^{1}H-NMR (δ, ppm, $CDCl_3$): 7.69–7.09 (4H, phenyl ring), 2.73–2.35 (9H, alkyl chain), 1.59–1.48 (9H, alkyl chain), 1.33–1.25 (60H, alkyl chain), 0.89–0.86 (9H, alkyl chain).

Bis(*t*-(dodecylthio)propan-2-yl) 4-dodecylphenylboronate (TSPB). Molecular formula: $C_{48}H_{91}BO_2S_2$. IR (KBr) (cm^{-1}): 2959.62m ($-CH_3$); 2928.79s, 2872.61m ($-CH_2-$); 1609.21w (C=C); 1460.11m, 1375.26m ($-CH_3$); 1342.51s ($-CH_2-$); 1319.25s (B–O); 759.51m (phenyl ring); 701.27w (C–B); 652.43w (C–S). ^{1}H-NMR (δ, ppm, $CDCl_3$): 8.15–7.11 (4H, phenyl ring), 2.70–2.34 (7H, alkyl ring), 1.53–1.21 (50H, alkyl chain), 0.87–0.83 (30H, alkyl chain).

2.2 Tribological evaluation

The tribological properties of TBPB, DSPB and TSPB as additives in mineral oil were investigated using a MMW-1 four-ball tester (manufactured by Ji'nan instrument manufacturer, China). The steel balls used in the tribological measurement are 12.7 mm in diameter and made of GCr 15 bearing steel with an HRC hardness of 59–61. General tribological tests were conducted under ambient conditions with a rotating speed of 1450 rpm for a time duration of 30 min.[5] The coefficient of friction (COF) was recorded automatically by a computer linked to the four-ball tester, and the values of the wear scar diameter (WSD) for the three lower balls were measured using an optical microscope with an accuracy of $\pm$0.01 mm. The maximum non-seizure loads (P_B values) tests of all additives were conducted according to the Chinese national standard GB12583-98, which is similar to ASTM D-2783.

2.3 Hydrolytic stability test

A wet heat treatment that causes accelerated hydrolysis was used in the hydrolytic stability test. Generally, 150 g of each lubricant sample (0.50 wt% or 2.0 wt% of each additive in the base oil) in a 200 mL beaker was placed in a hot and humid oven (50 $\pm$ 2 °C, relative humidity >95%). Each lubricant sample was monitored hourly until there was precipitation observed or the oil was no longer transparent, which indicates the hydrolysis of the additive. The final time was recorded as a parameter for describing the hydrolytic stability of each additive.[21]

2.4 Surface analysis

A NanoScope IIIa atomic force microscope (Digital Instruments) was used to investigate the morphology of the tribosurfaces on the steel balls. The surface roughness (root mean square, S_q) of the anti-wear films was calculated by Image Analysis 2 software.

XANES data were collected at the Beijing Synchrotron Radiation Facility (BSRF), which is situated at the 2.2 GeV storage ring, Beijing Electron Positron Collider (BEPC).[22] The K-edge spectra of boron were recorded using the soft X-ray optics beamline in the total electron yield (TEY) mode with a resolution of 1000 ($E/\Delta E$). This beamline is monochromatized by a Monk–Gillieson monochromator using 800 mm^{-1} gratings to cover the region of 190–210 eV. The K-edge spectra of sulfur were obtained using the mid-energy spectroscopy beamline in the fluorescence yield (FY) mode with a double-crystal monochromator covering the energy of 2450–2500 eV. Both the K-edge of boron and sulfur provide chemical information about the surface of the reaction film. The thermal films were prepared under the following parameters: steel ball; additive concentration, 2.0 wt%; temperature, 150 °C; and time, 6 h. The tribofilms for XANES evaluation were generated from the tribological tests (the upper balls). All the examined samples were gently rinsed in petroleum ether prior to XANES analyses.[22] Some model compounds were also scanned and recorded for the purpose of identification and comparison.

3. Results and discussion

3.1 Hydrolytic stabilities of synthesized additives

The hydrolytic stabilities of TBPB, DSPB and TSPB are listed in Table 3, and for comparison, the additives TB (tributyl borate) and NBO (N-containing borate ester)[23] have also been listed. Overall, the hydrolytic stability of each additive decreases with increase in concentration, which is ascribed to the high reaction probability between the additive molecule and water when the additive concentration is high. As shown in Table 3, at 0.5 wt% and 2.0 wt% of TB, the solutions start to hydrolyze in a very short amount of time of 10 h and 2 h, respectively; however, NBO exhibits better hydrolytic stability than TB due to the stabilization of the boron atom by coordination with nitrogen in its molecular structure.[23] The hydrolytic stabilities of the synthesized compounds is considerably improved compared with that of TB and NBO, which can be attributed to the following two major points: (1) the improved stability of boron due the phenyl group through p-π conjugation, and (2) the presence of a long alkyl chain that prevents a nucleophilic attack by water. This is further supported by the experimental observation that TSPB is more hydrolytically stable than DSPB and TBPB because its alkyl chain is longer (12C) than that of TBPB (4C) and more complicated (*t*-dodecyl) than that of DSPB

Table 3 The hydrolytic stability of boric esters

	0.5 wt%	2.0 wt%
TB	10 h	2 h
NBO	48 h	16 h
TBPB	312 h	89 h
DSPB	475 h	282 h
TSPB	599 h	496 h

(*n*-dodecyl). Therefore, the order of hydrolytic stabilities of the synthesized additives is TSPB > DSPB > TBPB. The observed experimental results and the trend of hydrolytic stabilities related to the molecular structures of the additives support our rationale for the molecular design. In addition, compared with a reported phenylboric ester,[21] the synthesized additives also show better hydrolytic stabilities due to the hydrophobic activity of the long alkyl chain that prevents the nucleophilic attack of the boron atom by water.

3.2 Anti-wear (AW) performance

Fig. 2 depicts the relationship between the additive concentration and the wear scar diameter (WSD) of each additive under 294 N. It is obvious that all the three additives are efficient in improving the anti-wear properties of the base oil at the tested concentration. Note that the anti-wear performance of DSPB is the best, while TBPB and TSPB are similar to each other. For DSPB, it can be seen that the WSD first decreases sharply when the additive is added to the base oil, and then with increasing additive concentration, the decrease in WSD becomes more gradual. In the case of TBPB and TSPB, the WSD also decreases rapidly when the additives are added, and then remains relatively stable with a slightly increasing trend. These results can be explained by two phenomena: the adsorption of the additive on the metal surface and the corrosive abrasion caused by the sulfur in the additive molecules.[24,25] Note that TSPB contains a branched chain structure, which leads to its poor adsorption on the metal surface; however, DSPB contains a more hydrophobic dodecyl group than TBPB, which leads to higher solubility in base oil, resulting in more the enhanced adsorption of DSPB on the metal surface. On the other hand, when the additive concentration is low, the corrosion of the S element can be ignored, but with increase in additive concentration, the corrosive abrasion becomes gradually more significant and finally counteracts the generation of a protective film, resulting in a dynamic equilibrium of abrasion. Furthermore, the difference in the anti-wear performance of the synthesized additives can be ascribed to the difference in the structure of the additive molecule.[26] As for the TSPB, due to the more serious corrosive abrasion caused by the more active sulfur in the branched chain *t*-dodecyl group than that of *n*-dodecyl group in DSPB,[26] the compactness of the protective film is impacted. However, for TBPB, as the *n*-butyl chain is short, associating with the element analysis results of the synthesized compounds, the content of sulfur is relatively high, which results in more corrosive abrasion compared with DSPB when the additives are at the same concentration.[7] Therefore, the WSD of TSPB and TBPB is higher than that of DSPB.

3.3 Friction-reducing performance

The coefficient of friction (COF) of the synthesized compounds at different concentrations under an applied load of 294 N is exhibited in Fig. 3. It can be seen from the curves that the three compounds show different friction-reducing properties. For DSPB, the COF first increases when the additive concentration is low, then decreases with an increase in the additive concentration, and finally remains relatively stable. These results suggest that the adsorbed additives interact with the freshly exposed worn surface on the friction pairs to form a protective adsorption film and/or reaction film. When the additive concentration is low, the protective film is not compact enough to resist the high shear force; thus, it could be damaged easily, whereas the shear strength is high, resulting in an increase in the COF.[28] With the increase in additive concentration from 0.5 wt% to 2.0 wt%, more additive molecules adsorb on the metal surface, which leads to the formation of a more compact protective film, and the adsorbed additive molecules act as an adsorption film, resulting in a decrease in the shear strength, and therefore the COF decreases. However, when the concentration is increased continuously, the COF increases slowly, which indicates that a component of the protective film is transformed with the increase in additive concentration. These details will be discussed in the surface analysis of the tribofilm. For TBPB and TSPB, the COF does not change much compared with the COF of the base oil, which indicates that the shear strength and roughness of the protective film remains relatively stable with the increase in additive concentration.

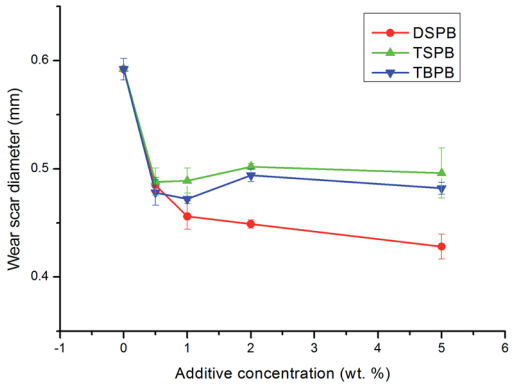

Fig. 2 The effect of additive concentration on the wear scar diameter (applied load, 294 N; rotary speed, 1450 rpm; duration, 30 min).

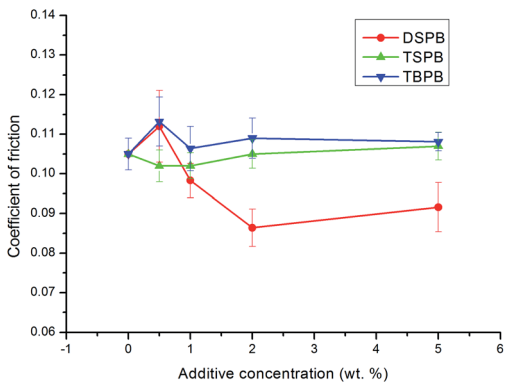

Fig. 3 The effect of additive concentration on the coefficient of friction (applied load, 294 N; rotary speed, 1450 rpm; duration, 30 min).

3.4 Extreme pressure (EP) performance

The effect of these S-containing long chain alkyl phenylboric esters under EP conditions was also investigated in this study. In general, the purpose of the EP additive is to provide added wear protection and anti-seizing properties to both metallic surfaces and lubricants under higher loads and temperatures.[26] The maximum non-seizure loads (P_B values) of the base oil (HVIW H150), 2.0 wt% DSPB, 2.0 wt% TSPB and 2.0 wt% TBPB in the base oil are presented in Fig. 4. Significantly, all of the synthesized additives are effective in enhancing the P_B value of the base oil. It is also clear that TBPB is better than DSPB in increasing the P_B value, because, according to the element analysis, the sulfur content in TBPB is higher than that of DSPB, leading to an increase in the maximum non-seizure load. Note that TSPB is the best among the three additives in EP performance. It has been reported that in the EP region, the surface layer is easily removed and a fresh metal surface is exposed continuously. Therefore, under these rigorous conditions, the additive that exhibits the best EP performance should be the one that reacts with the newly formed metal surface to generate the thickest protective film.[29] Therefore, TBPB exhibits better EP performance than DSPB due to its higher sulfur content; moreover, the P_B value is also related to the reactivity of sulfur. It is known that the reactivity of *t*-dodecylthio group is higher than that of the *n*-dodecylthio group.[27] Upon the generation of high shear forces and triboheat due to the EP conditions, the C–S bond is cleaved and the *t*-dodecylthio group is more likely to react with the freshly exposed metal surface to form a protective film, resulting in an improvement in the maximum non-seizure load. However, although the reactivity of TSPB is higher than of DSPB, the anti-wear property of TSPB does not perform better than that of DSPB, which is ascribed to a limitation of the branched group with respect to access to the friction pairs. Therefore, TSPB performs well in the extreme pressure property (P_B value), but exhibits relatively poor performance in anti-wear property.

As discussed above, all the three synthesized additives exhibit good anti-wear and relatively high EP properties, especially DSPB, which also exhibits friction-reducing performance. These results make us believe that there are tribological reactions occurring on the metal surface of the friction pairs during the rubbing processes. Thus, formation of a protective film covering the metal surface prevents direct metal-to-metal contact between the surface asperities. The difference in the components and the surface morphology of the protective film may be responsible for the difference in the tribological performance. Therefore, it is worthwhile to investigate the nature of the protective film by performing surface analysis of the worn surface.

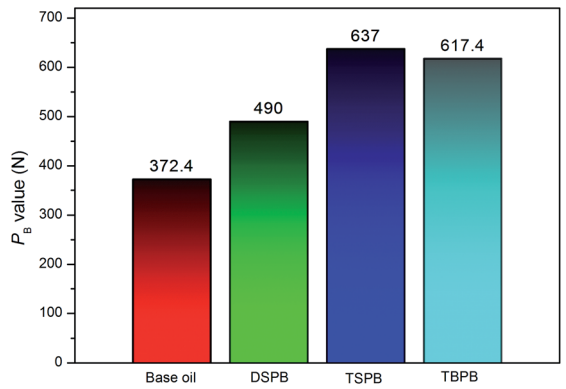

Fig. 4 Maximum non-seizure loads (P_B values) of the synthesized compounds (four-ball machine, rotation velocity of 1760 rpm for 10 s).

3.5 Surface analysis

3.5.1 Atomic force microscopy (AFM) analysis. AFM was used to examine the general morphology of the reaction films generated from the additives under AW conditions. The 2D and 3D AFM topography images of tribofilms generated from the synthesized additives are shown in Fig. 5 and 6. In comparison with the 2D and 3D AFM images of tribofilms generated from the synthesized additives, it clearly reflects that the tribofilms are quite heterogeneous. They are composed of large pads and are elongated and orientated in the sliding direction, which is several tens of microns long and several microns wide. This phenomenon is similar to the tribofilm lubricated with ZDDPs,

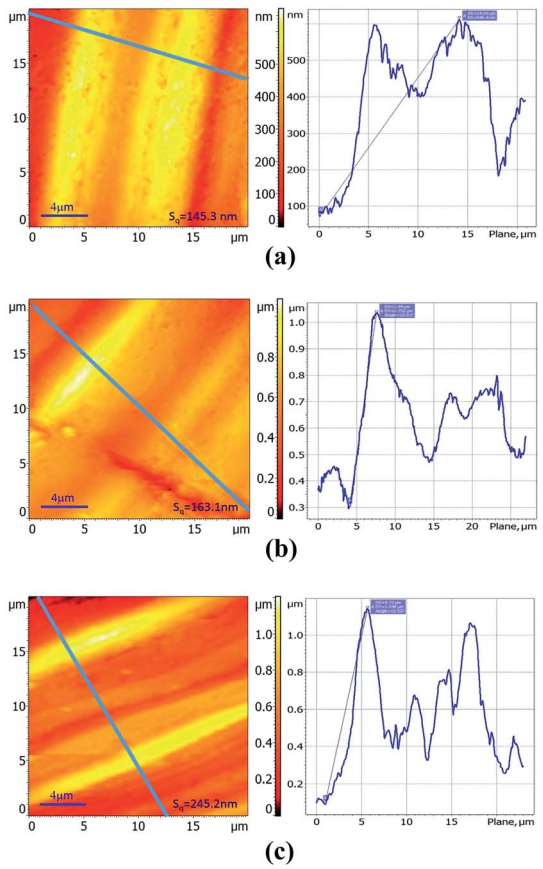

Fig. 5 AFM topography images (20 × 20 μm) of boundary films generated from the synthesized additives along with the topographic profiles images taken along the dotted lines: (a) DSPB; (b) TSPB; (c) TBPB (2.0 wt% additive in base oil, applied load, 294 N; rotary speed, 1450 rpm; duration, 30 min).

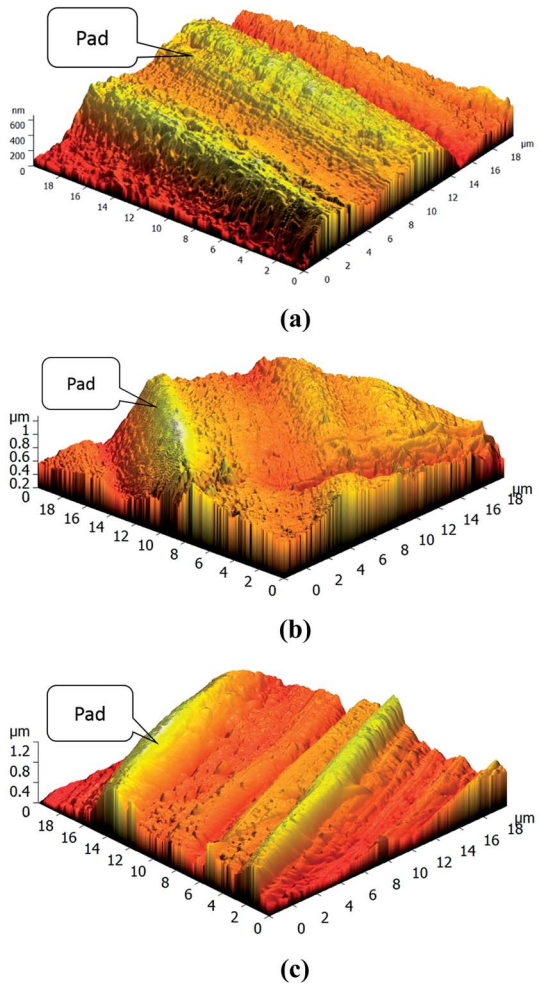

Fig. 6 3D topography images (20 × 20 μm) of boundary films generated from the synthesized additives: (a) DSPB; (b) TSPB; (c) TBPB (2.0 wt% additive in base oil, applied load, 294 N; rotary speed, 1450 rpm; duration, 30 min).

which had been reported previously.[30–32] The pads formed by DSPB are larger and more compact than those of TSPB and TBPB, which explains why DSPB exhibits better anti-wear properties (Fig. 2). The topography images also allow for an accurate determination of the height profile of the anti-wear pads[32,33] and the roughness of the metal surface of friction pairs.[34] A cross-sectional analysis of the pad was performed along the dotted line, which is shown in Fig. 5. The anti-wear pads of DSPB, TSPB and TBPB were found to be 540.4 nm, 732.0 nm and 1048.0 nm thick, respectively. Together with the EP properties presented in Fig. 4 and the 3D AFM topography images, the results indicate that the TSPB and TBPB are more active in reacting with the fresh metal surface to generate a thicker protective film, which leads to better EP properties. Despite the thicker pad of TBPB, the more corrosive abrasion by sulfur results in a slightly worse EP performance compared with that of TSPB. Moreover, due to the corrosive abrasion, the compactness of the protective film is impacted, which leads to smaller and more sparse pads, resulting in poor anti-wear properties. The values of surface roughness (S_q) of DSPB, TSPB and DSPB are 145.3 nm, 163.1 nm and 245.2 nm, respectively. This result demonstrates that a smoother metal surface leads to a lower COF, which agrees with the data on the friction-reducing performance shown in Fig. 3.

3.5.2 XANES Analysis of thermal film and tribofilm. The AFM analysis of the tribofilms indicates the formation of a protective film by the synthesized additives. In order to obtain detailed information on the chemical state of the protective film on the surface of the frictional pairs, X-ray absorption near edge structure (XANES) spectroscopy was used to investigate the thermal films and tribofilms generated from the synthesized additives in base oil. Several model compounds were also used for comparison to determine the chemical state of the film.

3.5.2.1 Thermal film. During the rubbing process, the reactions between the adsorbed additives and friction pairs proceed with the help of triboheat, exoelectron, and a catalytic effect of the renascent metal surface.[35] It is generally accepted that thermal films may provide additional information about the reactions taking place prior to friction. Note that the temperature at the contact point between the frictional pairs is about 150 °C below moderate AW conditions;[36] therefore, the thermal films were prepared at the temperature of 150 °C. The B K-edge (TEY) and S K-edge (FY) XANES spectra of the thermal films generated from synthesized additives at 2.0 wt% along with some model compounds are presented in Fig. 7. Their peak positions along with some relevant model compounds are listed in Tables 4 and 5. Compared with the model compounds, the boron element in the synthesized additives has mainly transformed into trigonal and tetragonal coordination boron, while the sulfur element has mostly transformed into a sulfate under the thermal oxidation conditions. Especially in DSPB, a small peak at 2473.7 eV, which corresponds to alkyl sulfide,[36] suggests that the triboheat generated from the friction pairs plays an important role in the formation of the protective films. Moreover, iron sulfide or iron disulfide is not found in the thermal films, which can be attributed to the cover of iron oxide on the surface of the sample, preventing active sulfur to react with the metal iron to form FeS or FeS_2.[22]

3.5.2.2 Tribofilm. The B K-edge (TEY) and S K-edge (FY) XANES spectra of the tribofilms generated from the synthesized additives at 0.5 wt% and 2.0 wt% along with some model compounds are presented in Fig. 8. Their peak positions along with some relevant model compounds are listed in Tables 6 and 7.

From the boron K-edge XANES spectra, it can be seen that the curves of the tribofilms generated from the synthesized compounds are similar to those of the thermal films, and they do not show a significant difference with increase in additive concentration except for the peak intensities. Similar to thermal films, the boron in the additive has mainly transformed into trigonal and tetragonal coordination boron by the triboheat, which also demonstrates that the triboheat generated from the friction pairs plays an important role in the formation of protective films. The result is consistent with the previous reports.[10,11,37] Furthermore, it can be seen that the peak intensity increases gradually with an increase in the additive

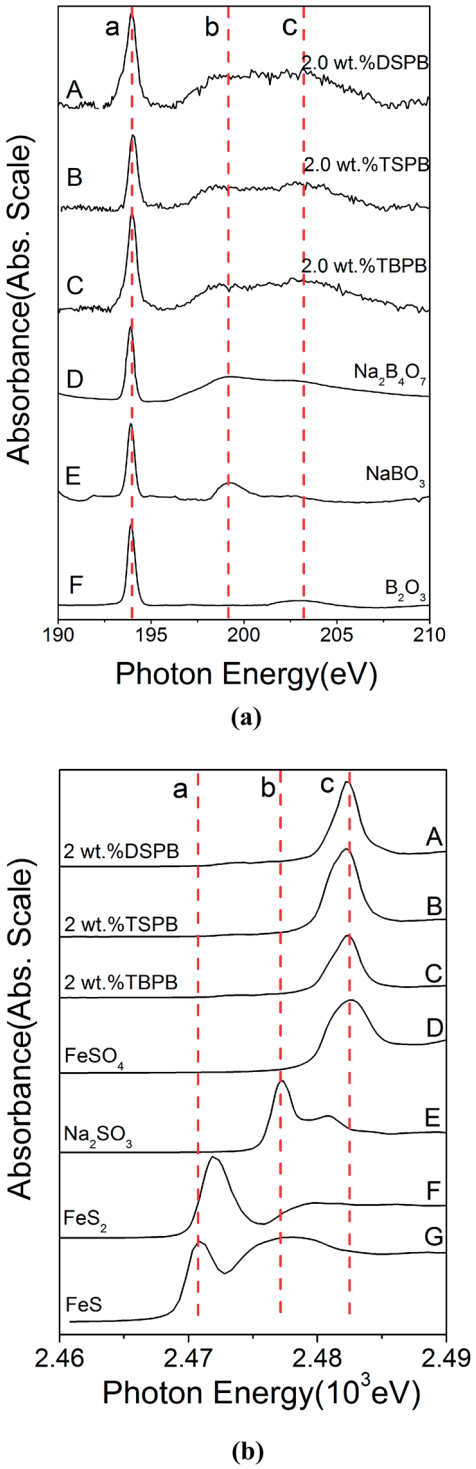

Fig. 7 XANES spectra of thermal films generated from synthesized additives and some model compounds: (a) B K-edge (TEY); (b) S K-edge (FY).

concentration, which suggests that the additional adsorbed additive molecules react with the metal surface to generate a thicker films. It is known that boron oxide is a very hard material,[38] which accounts for the decrease in the WSD and an increase in the COF when the additive concentration is high. Because harder materials are generated, the protective film becomes more compact to prevent direct contact with the metal surface leading to a decline in the WSD; moreover, the roughness of the surface increases, resulting in an increase in the COF.

Table 4 Peak positions of B K-edge (TEY) spectra of thermal films and model compounds

K-edge			
	a	*b*	*c*
Samples			
2.0 wt% DSPB	193.9	199.2	203.2
2.0 wt% TSPB	193.9	199.2	203.2
2.0 wt% TBPB	193.9	199.2	203.2
Model compounds			
$Na_2B_4O_7$	193.9	199.2	203.2
$NaBO_3$	193.9	199.2	
B_2O_3	193.9		203.2

Table 5 Peak positions of S K-edge (FY) spectra of thermal films along with model compounds

K-edge					
	a	*b*	*c*	*d*	*e*
Samples					
2.0 wt% DSPB			2473.7		2482.4
2.0 wt% TSPB					2482.2
2.0 wt% TBPB					2482.4
Model compounds					
FeS	2470.7			2477.2	
FeS_2		2472.0			
Na_2SO_3				2477.2	
$FeSO_4$					2482.4

With regard to the sulfur K-edge XANES spectra, it is apparent that the film chemistry changes under the boundary conditions of high shear force and triboheat generated from the rubbing process. This can be explained by the fact that during the sliding process, the fresh metal surface was exposed continuously and therefore the active sulfur could react with the fresh metal surface.[22] There are three apparent peaks observed at 2470.7 eV, 2477.2 eV and 2482.4 eV. According to the spectra of model compounds, it can be seen that the tribofilm is mainly composed of iron sulfide and iron sulfate. In addition, the peak at 2472.0 eV, attributed to iron disulfide can also be found, although it is not significant. For DSPB, it is obvious that the peak of sulfide and disulfide is weaker than that of TSPB, while the peak of sulfate is stronger. The sulfide and disulfide films are easily worn down during the rubbing processes, which leads to inferior anti-wear performance of TSPB.[26] Although the peak of the sulfide and disulfide of TBPB is weak (panel F), due to the corrosion caused by the high content of sulfur, the anti-wear performance of TBPB is not as good as that of DSPB. This explains why the anti-wear performance of DSPB is better than that of TSPB and TBPB.

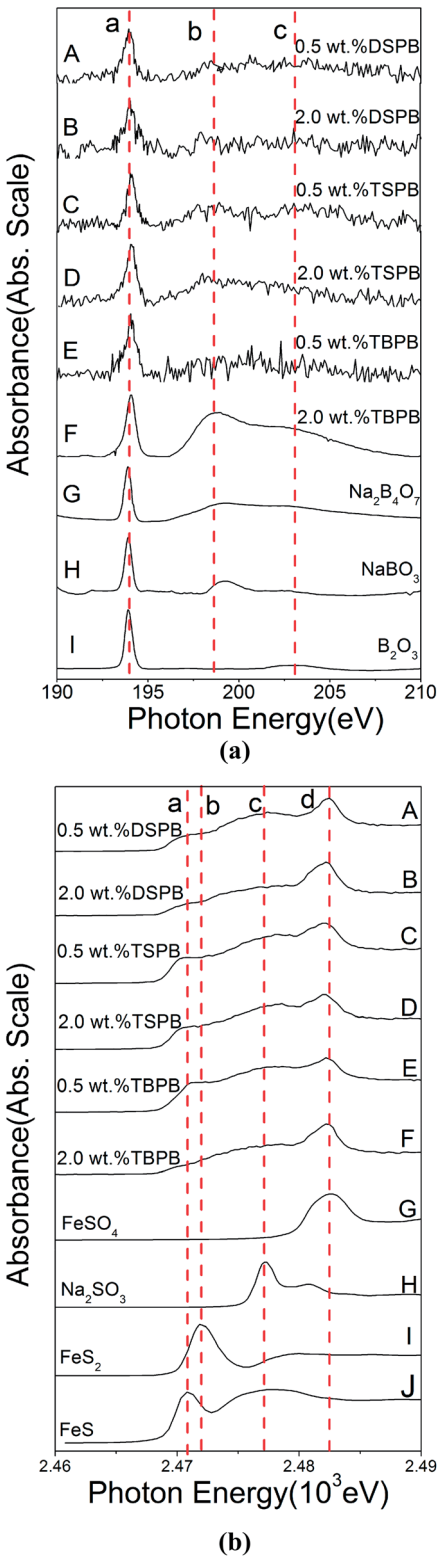

Fig. 8 XANES spectra of tribofilms generated from synthesized additives and some model compounds: (a) B K-edge (TEY); (b) S K-edge (FY) (applied load, 294 N; rotary speed, 1450 rpm; duration, 30 min).

3.6 Discussion

Based on the hydrolytic stability test, tribological evaluation and surface analysis by XANES and AFM, it can be inferred that under the boundary lubrication conditions, a complicated tribofilm is generated from the synthesized additives, which prevents direct contact between the asperities on the surface of friction pairs. As for the hydrolytic stability, directly linking a long chain alkyl phenyl with boron is an efficient method to enhance the hydrolytic stability of the borate ester. Moreover, the structure of the group around the boron element also leads to hydrolytic stability. A complicated group is beneficial for improving the hydrolytic stability of the borate ester. However, for the tribological properties, the amount and activity of the sulfur have a great influence on the AW and EP performance. Furthermore, there is an equilibrium for the amount of sulfur contained in the additive molecule because of corrosive abrasion. With regard to the surface analysis of XANES and AFM, it can be seen that the tribofilm consists of large pads on the asperities of the metal surface, composed of trigonal and tetragonal coordination boron, iron sulfide and disulfide, and iron sulfate. The compactness and roughness of the tribofilm correspond to the AW and friction-reducing properties. A more compact and smooth tribofilm results in better AW and friction-reducing performance.

Table 6 Peak positions of B K-edge (TEY) spectra for thermal films and model compounds

K-edge			
	a	*b*	*c*
Samples			
0.5 wt% DSPB	193.9	199.2	203.2
2.0 wt% DSPB	193.9	199.2	203.2
0.5 wt% TSPB	193.9	199.2	203.2
2.0 wt% TSPB	193.9	199.2	203.2
0.5 wt% TBPB	193.9	199.2	203.2
2.0 wt% TBPB	193.9	199.2	203.2
Model compounds			
$Na_2B_4O_7$	193.9	199.2	203.2
$NaBO_3$	193.9	199.2	
B_2O_3	193.9		203.2

Table 7 Peak positions of S K-edge (FY) spectra for thermal films and model compounds

K-edge				
	a	*b*	*c*	*d*
Samples				
0.5 wt.% DSPB	2470.7	2472.0	2477.2	2482.4
2.0 wt.% DSPB	2470.7	2472.0	2477.2	2482.4
0.5 wt.% TSPB	2470.7	2472.0	2477.2	2482.4
2.0 wt.% TSPB	2470.7	2472.0	2477.2	2482.2
0.5 wt.% TBPB	2470.7	2472.0	2477.2	2482.4
2.0 wt.% TBPB	2470.7	2472.0	2477.2	2482.4
Model compounds				
FeS	2470.7		2477.2	
FeS_2		2472.0		
Na_2SO_3			2477.2	
$FeSO_4$				2482.4

4. Conclusions

The hydrolytic stability, tribological performance and wear behaviour of three S-containing alkyl phenylboric esters have been investigated and discussed. The results can be summarized as follows:

• The three synthesized compounds used as additive in base oil exhibit superior hydrolytic stability compared with tributyl borate, NBO and phenylboric ester reported previously. This demonstrates that the designed molecular structure (by introducing long chain alkylphenyl group to conjugate with the electron-deficient boron) is effective on enhancing the hydrolytic stability of borate ester. Moreover, the structure of the group around the boron element also affects the hydrolytic stability.

• The synthesized compounds possess relatively good antiwear performance as additives in base oil, especially DSPB, which also has friction-reducing properties. Combined with its excellent hydrolytic stability, DSPB is a promising candidate for future lubricant additives.

• The AFM analysis of tribofilm clearly demonstrates that the compactness and smoothness of DSPB is better than that of TSPB and TBPB, which leads to the better AW and friction-reducing performance.

• The boron and sulfur K-edge XANES analysis reveal that the thermal film is mainly composed of trigonal and tetragonal coordination boron, and iron sulfate, while the tribofilm consists of trigonal and tetragonal coordination boron, iron sulfide and disulfide, and iron sulfate; moreover, the triboheat is a key factor for the boron to generate tribofilm.

Acknowledgements

The authors are grateful to the National Natural Science Foundation of China (grant no. 21272157), the Beijing Synchrotron Radiation Facility (Grant no. SR06033) and the open projects of the Key State Lab of Solid Lubrication in Lanzhou of China (Grant no. 1205) for financially supporting of the work reported here. We are grateful to the Beijing Synchrotron Radiation Facility for the XANES analysis.

Notes and references

1 W. J. Bartz, *Tribol. Int.*, 2006, **39**, 728–733.
2 K. Holmberg, P. Andersson and A. Erdemir, *Tribol. Int.*, 2012, **47**, 221–234.
3 F. U. Shah, S. Glavatskih, E. Hoglund, M. Lindberg and O. N. Antzutkin, *ACS Appl. Mater. Interfaces*, 2011, **3**, 956–968.
4 N. J. Mosey, T. K. Woo, M. Kasrai, P. R. Norton, G. M. Bancroft and M. H. Muser, *Tribol. Lett.*, 2006, **24**, 105–114.
5 J. Li, X. Xu, Y. Wang and T. Ren, *Tribol. Int.*, 2010, **43**, 1048–1053.
6 F. U. Shah, S. Glavatskih and O. N. Antzutkin, *Tribol. Lett.*, 2011, **45**, 67–78.
7 H. Spikes, *Lubr. Sci.*, 2008, **20**, 103–136.
8 B. A. Baldwin, *Wear*, 1977, **45**, 345–353.
9 R. Choudhary and P. Pande, *Lubr. Sci.*, 2002, **14**, 211–222.
10 A. Papay, *Lubr. Sci.*, 1998, **10**, 209–224.
11 D. Philippon, M. I. Barros-Bouchet, O. Lerasle, T. Mogne and J. M. Martin, *Tribol. Lett.*, 2010, **41**, 73–82.
12 R. Kapadia, R. Glyde and Y. Wu, *Tribol. Int.*, 2007, **40**, 1667–1679.
13 G. Shen, Z. Zheng, Y. Wan, X. Xu, L. Cao, Q. Yue, T. Sun and A. Liu, *Wear*, 2000, **246**, 55–58.
14 Z. Zheng, G. Shen, Y. Wan, L. Cao, X. Xu, Q. Yue and T. Sun, *Wear*, 1998, **222**, 135–144.
15 F. U. Shah, S. Glavatskih and O. N. Antzutkin, *Tribol. Lett.*, 2013, **51**, 281–301.
16 Y. Sun, L. Hu and Q. Xue, *Wear*, 2009, **266**, 917–924.
17 J. Zhang, W. Liu and Q. Xue, *Wear*, 1999, **224**, 68–72.
18 Q. Gong, W. Liu and C. Ye, *Tribology*, 2002, **22**, 360–363.
19 M. A. Hall, J. Xi, C. Lor, S. Dai, R. Pearce, W. P. Dailey and R. G. Eckenhoff, *J. Med. Chem.*, 2010, **53**, 5667–5675.
20 J. X. Cai, A. Farhat, P. B. Tsitovitch, V. Bodani, R. D. Toogood and R. S. Murphy, *J. Photochem. Photobiol., A*, 2010, **212**, 176–182.
21 Y. Wang, J. Li, Z. He and T. Ren, *Proc. Inst. Mech. Eng., Part J*, 2008, **222**, 133–140.
22 J. Li, H. Ma, T. Ren, Y. Zhao, L. Zheng, C. Ma and Y. Han, *Appl. Surf. Sci.*, 2008, **254**, 7232–7236.
23 J. Yan, X. Bai, T. Ren and X. Zeng, *Petroleum Products Application Research*, 2012, **30**, 109–111 (in Chinese).
24 J. W. You, F. F. Li and B. S. Chen, *China Pet. Process. Petrochem. Technol.*, 2010, **12**, 43–48.
25 H. Wu, J. Li, H. Ma and T. Ren, *Surf. Interface Anal.*, 2009, **41**, 151–156.
26 H. Chen, J. Yan, T. Ren, Y. Zhao and L. Zheng, *Tribol. Lett.*, 2012, **45**, 465–476.
27 D. Li, X. Yu and Y. Dong, *Appl. Surf. Sci.*, 2007, **253**, 4182–4187.
28 S. Aoki, A. Suzuki and M. Masuko, *Proc. Inst. Mech. Eng., Part J*, 2006, **220**, 343–351.
29 X. Zeng, J. Li, X. Wu, T. Ren and W. Liu, *Tribol. Int.*, 2007, **40**, 560–566.
30 M. N. Najman, M. Kasrai and G. M. Bancroft, *Tribol. Lett.*, 2004, **17**, 217–229.
31 M. A. Nicholls, G. M. Bancroft, M. Kasrai, P. R. Norton, B. H. Frazer and G. De Stasio, *Tribol. Lett.*, 2005, **18**, 453–462.
32 M. A. Nicholls, G. M. Bancroft, P. R. Norton, M. Kasrai, G. De Stasio, B. H. Frazer and L. M. Wiese, *Tribol. Lett.*, 2004, **17**, 245–259.
33 B. Vengudusamy, A. Grafl, F. Novotny-Farkas, T. Schimmel and K. Adam, *Tribol. Int.*, 2013, **67**, 199–210.
34 V. Jaiswal, R. B. Rastogi, R. Kumar, L. Singh and K. D. Mandal, *J. Mater. Chem. A*, 2014, **2**, 375.
35 C. McFadden, C. Soto and N. D. Spencer, *Tribol. Int.*, 1997, **30**, 881–888.
36 M. N. Najman, M. Kasrai and G. M. Bancroft, *Tribol. Lett.*, 2003, **14**, 225–235.
37 J. Yan, X. Zeng, E. van der Heide and T. Ren, *Tribol. Int.*, 2014, **71**, 149–157.
38 P. Ball, *Nat. Mater.*, 2010, **9**, 6.

